Available online at www.eccomasproceedia.org
Eccomas Proceedia COMPDYN (2017) 20-36

ECCOMAS
Proceedia

COMPDYN 2017
6th ECCOMAS Thematic Conference on
Computational Methods in Structural Dynamics and Earthquake Engineering
M. Papadrakakis, M. Fragiadakis (eds.)
Rhodes Island, Greece, 15–17 June 2017

HIGHER ORDER BEAM ELEMENT FOR THE LOCAL BUCKLING ANALYSIS OF BEAMS

Amalia K. Argyridi[1] and Evangelos J. Sapountzakis[2]

[1] Institute of Structural Analysis and Antiseismic Research, School of Civil Engineering
National Technical University of Athens, Athens, 15780, Greece
e-mail: a.argyridi@gmail.com

[2] Institute of Structural Analysis and Antiseismic Research, School of Civil Engineering
National Technical University of Athens , Athens, 15780, Greece
e-mail: cvsapoun@central.ntua.gr, web page: http://users.ntua.gr/cvsapoun/

Keywords: Distortion, Warping, In-plane deformation, Out-of-plane deformation, Buckling, Beam.

Abstract. *In this paper, a higher order beam theory is employed for local buckling analysis of beams of arbitrarily shaped, homogeneous cross-section, taking into account warping and distortional phenomena due to shear, flexure and torsion. The beam is subjected to arbitrary axial, transverse and/or torsional concentrated or distributed load, while its edges are restrained by the most general linear boundary conditions. The analysis consists of two stages. In the first stage, where the Boundary Element Method is employed, a cross sectional analysis is performed based on the so-called sequential equilibrium scheme establishing the possible in-plane (distortion) and out-of-plane (warping) deformation patterns of the cross section. In the second stage, where the Finite Element Method is employed, the extracted deformation patterns are included in the buckling analysis multiplied by respective independent parameters expressing their contribution to the beam deformation. The four rigid body displacements of the cross section together with the aforementioned independent parameters consist the degrees of freedom of the beam. The finite element equations are formulated with respect to the displacements and the independent warping and distortional parameters. The buckling load is calculated and compared with beam and 3d solid analysis results in order to validate the method and demonstrate its efficiency and accuracy.*

Peer-review under responsibility of the organizing committee of COMPDYN 2017.
doi: 10.7712/120117.5407.17453

1 INTRODUCTION

In most cases in the analysis of beam-like structures, Euler – Bernoulli beam theory assumptions are adopted, while in the case of non-negligible shear deformation effect, these assumptions are relaxed by using Timoshenko beam theory. However, both theories maintain the assumptions that plane cross sections remain plane (no out-of-plane deformation) and that their shape does not change after deformation (no in-plane deformation). In order to take into account shear lag effects in the context of a beam theory, the inclusion of non-uniform warping is necessary, relaxing the assumption of plane cross section. The shear flow associated with non-uniform warping leads also to in plane deformation of the cross section, relaxing the assumption that the cross section shape does not change after deformation. For this purpose the so-called higher order beam theories have been developed taking into account shear lag [1] and distortional (in-plane deformation) effects [2].

Elastic stability of beams is one of the most important criteria in the design of structures. In this paper, a higher order beam theory is employed for local buckling analysis [3] of beams of arbitrarily shaped, homogeneous cross-section [4], taking into account warping and distortional phenomena due to shear, flexure and torsion. The beam is subjected to arbitrary axial, transverse and/or torsional concentrated or distributed load, while its edges are restrained by the most general linear boundary conditions. The analysis consists of two stages. In the first stage, where the Boundary Element Method (BEM) is employed, a cross sectional analysis is performed based on the so-called sequential equilibrium scheme establishing the possible in-plane (distortion) and out-of-plane (warping) deformation patterns of the cross section [4]. In the second stage, where the Finite Element Method (FEM) is employed, the extracted deformation patterns are included in the buckling analysis multiplied by respective independent parameters expressing their contribution to the beam deformation. The four rigid body displacements of the cross section together with the aforementioned independent parameters consist the degrees of freedom of the beam. The finite element equations are formulated with respect to the displacements and the independent warping and distortional parameters. The buckling load is calculated and compared with beam and 3d solid analysis results in order to validate the method and demonstrate its efficiency and accuracy.

The essential features and novel aspects of the proposed formulation compared with previous ones are summarized as follows.

i) It takes into account distortional effects (due to shear, flexure and torsion) in local buckling analysis of non-symmetric, prismatic beams.
ii) It performs buckling (global and local) analysis based on a higher-order beam theory that is of increased interest due to its important advantages over refined approaches such as 3-D solutions.
iii) The influence of Poisson ratio is taken into account in the buckling analysis of beams.
iv) The beam is supported by the most general linear boundary conditions including elastic support or restraint.

2 STATEMENT OF THE PROBLEM

2.1 Displacement, strain and stress components

Let us consider a prismatic beam of length L (Figure 1a), of constant arbitrary cross-section A . The cross section consists of a homogeneous material, with modulus of elasticity E and poisson ratio ν, occupying the two-dimensional multiply connected region Ω of the y,z plane (Figure 1b) and is bounded by the $\Gamma_j \left(j=1,2,...,K \right)$ boundary curves, which are piecewise smooth, i.e. they may have a finite number of corners. In Figure 1b CYZ is the coordinate system through the cross section's centroid C, while y_C, z_C are its coordinates with respect to Syz principal shear system of axes through the cross section's shear center S.

The beam can be supported by the most general linear boundary conditions and is subjected to the combined action of the arbitrarily distributed or concentrated axial loading $p_x(X)$ along X direction, transverse loading $p_y(x)$ and $p_z(x)$ along the y, z directions, respectively, twisting moment $m_x(x)$ along x direction, bending moments $m_Y^P(x)$, $m_Z^P(x)$ along Y, Z directions, respectively, as well as bending $m_{\varphi_Y^S}(x)$, $m_{\varphi_Z^S}(x)$ and primary and secondary torsional $m_{\varphi_x^P}(x)$, $m_{\varphi_x^S}(x)$ warping moments, and higher moments $m_{Dx}^P(x)$, $m_{Dx}^S(x)$, $m_{DY}^P(x)$, $m_{DY}^S(x)$, $m_{DZ}^P(x)$, $m_{DZ}^S(x)$ which in what follows will be referred to as distortional moments. The displacement field is considered consisting of two parts i.e. the rigid body part and end the effects part (warping and distortional effects). Under the aforementioned loading and assuming that there is an event that causes instability to the beam, the displacement field of the beamwith respect to the Syz system of axes at the buckled configuration is given as

$$\begin{aligned}\bar{u}(x,y,z) = {} & \overbrace{u(x)}^{\text{Rigid Body Motion}} + \overbrace{\bar{\eta}_Y^P(x)\phi_Y^P(y,z) + \bar{\eta}_Z^P(x)\phi_Z^P(y,z) + \bar{\eta}_x^P(x)\phi_x^P(y,z)}^{\text{Primary Warping}} + \\ & + \overbrace{\bar{\eta}_Y^S(x)\phi_Y^S(y,z) + \bar{\eta}_Z^S(x)\phi_Z^S(y,z) + \bar{\eta}_x^S(x)\phi_x^S(y,z)}^{\text{Secondary Warping}}\end{aligned} \tag{1a}$$

$$\begin{aligned}\bar{v}(x,y,z) = {} & \overbrace{v(x) - z\cdot\sin(\theta_x(x)) - y\cdot(1-\cos(\theta_x(x)))}^{\text{Rigid Body Motion}} + \\ & + \overbrace{v_Y^P(y,z)z_Y^P(x) + v_Z^P(y,z)\;z_Z^P(x) + v_x^P(y,z)\;z_x^P(x)}^{\text{Primary Distortion (component along Y axis)}} + \\ & + \overbrace{v_Y^S(y,z)z_Y^S(x) + v_Z^S(y,z)\;z_Z^S(x) + v_x^S(y,z)\;z_x^S(x)}^{\text{Secondray Distortion (component along Y axis)}}\end{aligned} \tag{1b}$$

$$\begin{aligned}\bar{w}(x,y,z) = {} & \overbrace{w(x) + y\cdot\sin(\theta_x(x)) - z\cdot(1-\cos(\theta_x(x)))}^{\text{Rigid Body Motion}} \\ & + \overbrace{w_Y^P(y,z)z_Y^P(x) + w_Z^P(y,z)\;z_Z^P(x) + w_x^P(y,z)\;z_x^P x(x)}^{\text{Primary Distortion (component along Z axis)}} \\ & + \overbrace{w_Y^S(y,z)z_Y^S(x) + w_Z^S(y,z)\;z_Z^S(x) + w_x^S(y,z)\;z_x^S x(x)}^{\text{Secondray Distortion (component along Z axis)}}\end{aligned} \tag{1c}$$

where

$$\phi_Y^P(y,z) = -Z \tag{1d}$$

$$\phi_Z^P(y,z) = -Y \tag{1e}$$

and

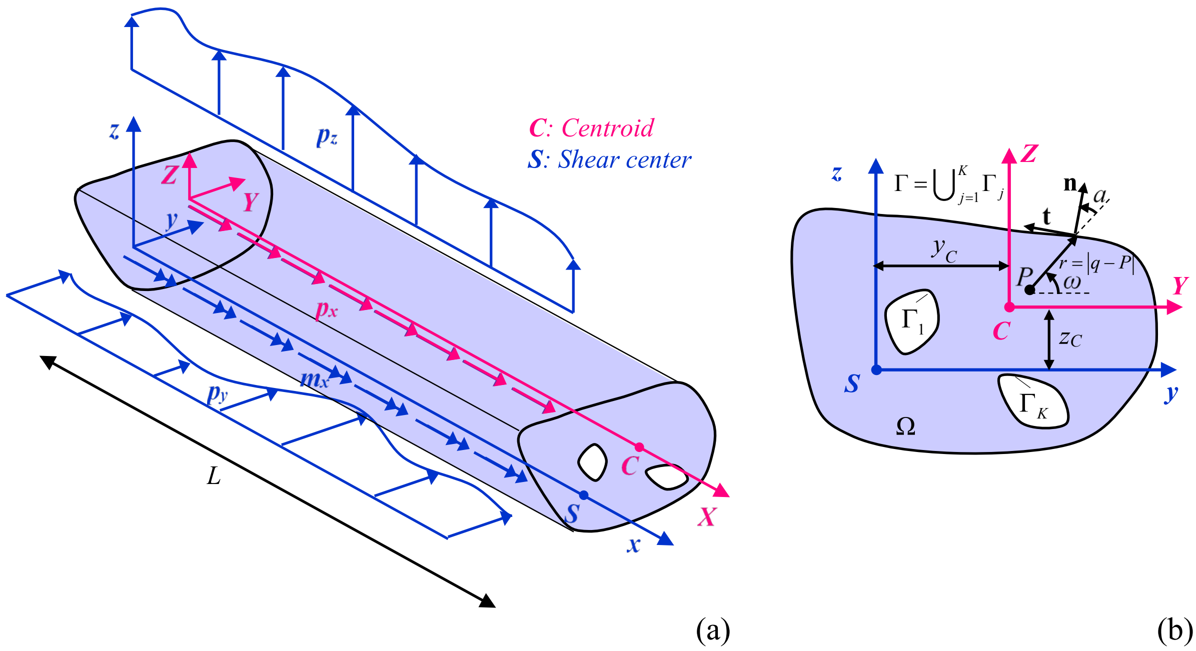

Figure 1: Prismatic beam under loading (a) with a homogeneous cross section of arbitrary shape occupying the two dimensional region Ω (b).

$$\bar{\eta}_Y^P = -\bar{\theta}_Y(x) = -\left(\theta_Z(x)\cdot\sin(\theta_x(x)) + \theta_Y(x)\cdot\cos(\theta_x(x))\right) \tag{1f}$$

$$\bar{\eta}_Z^P = \bar{\theta}_Z(x) = \theta_Z(x)\cdot\cos(\theta_x(x)) - \theta_Y(x)\cdot\sin(\theta_x(x)) \tag{1g}$$

$$\theta_Y^P(x) = \eta_Y^P(x) \qquad \theta_Z^P(x) = \eta_Z^P(x) \qquad \bar{\eta}_x^P(x) = \eta_x^P(x) \tag{1h,i,j}$$

$$\bar{\eta}_Y^S(x) = \eta_Y^S(x) \qquad \bar{\eta}_Z^S(x) = \eta_Z^S(x) \qquad \bar{\eta}_x^S(x) = \eta_x^S(x) \tag{1k,l,m}$$

where $\bar{u}$, $\bar{v}$, $\bar{w}$ are the axial and transverse beam displacement components with respect to the $Sxyz$ system of axes. Moreover, $v(x)$, $w(x)$ describe the deflection of the center of twist S, while $u(x)$ denotes the "average" axial displacement of the cross section. $\bar{\eta}_i^j(x)$ ($i = Y, Z, x$ and $j = P, S$) are the independent warping parameters introduced to describe the nonuniform distribution of primary ($j = P$) or secondary ($j = S$) warping due to bending about Y ($i = Y$) or Z ($i = Z$) axis or due to torsion about x axis ($i = x$). $z_i^j(x)$ ($i = Y, Z, x$ and $j = P, S$) are the independent distortional parameters introduced to describe the nonuniform distribution of primary ($j = P$) or secondary ($j = S$) distortion due to bending about Y ($i = Y$) or Z ($i = Z$) or due to torsion about x axis ($i = x$). $\bar{\eta}_Y^P(x)$ and $\bar{\eta}_Z^P(x)$ are related with the respective bending rotations $\theta_Y(x)$, $\theta_Z(x)$ due to bending about the Y, Z axes, according to Eqs. (1f-g). For generality purposes $\theta_Y(x)$, $\theta_Z(x)$ will be referred as $\eta_Y^P(x), \eta_Z^P(x)$ (Eqs. (1h,i)) and the rest of independent warping parameters i.e. $\bar{\eta}_i^j(x)$ ($\bar{\eta}_x^P(x)$ and $\bar{\eta}_i^j(x)$ for $i = Y, Z, x$ and $j = S$) will be referred as $\eta_i^j(x)$(Eqs. (1j-m)) . Despite the fact that $\bar{\eta}_Y^P(x)$ and $\bar{\eta}_Z^P(x)$ are basically rigid body rotations, they are referred as primary independent warping parameters, for generality purposes, because they correspond to z_Y^P and

z_Z^P which are the primary independent distortional parameters introduced to describe the nonuniform distribution of primary flexural distortion due to bending about the centroidal Y, Z axes. $\phi_i^j(y,z)$ ($i=Y,Z,x$ and $j=P,S$) are the primary ($j=P$) or secondary ($j=S$) warping functions related with shear due to bending about Y ($i=Y$) or Z ($i=Z$) axis or torsion about x axis ($i=x$). $v_i^j(y,z)$ ($i=Y,Z,x$ and $j=P,S$) are the primary ($j=P$) or secondary ($j=S$) components of distortional functions along Y axis related with shear due to bending about Y ($i=Y$) or Z ($i=Z$) axis or torsion about x axis ($i=x$). $w_i^j(y,z)$ ($i=Y,Z,x$ and $j=P,S$) are the primary ($j=P$) or secondary ($j=S$) components of distortional functions along Z axis related with shear due to bending about Y ($i=Y$) or Z ($i=Z$) axis or torsion about x axis ($i=x$). It holds that $Z=z-z_C$, $Y=y-y_C$.

Substituting Eqs.(1a)-(1c) in the non-linear (Green) strain-displacement relations

$$\varepsilon_{xx}=\frac{\partial\bar{u}}{\partial x}+\frac{1}{2}\left[\left(\frac{\partial\bar{u}}{\partial x}\right)^2+\left(\frac{\partial\bar{v}}{\partial x}\right)^2+\left(\frac{\partial\bar{w}}{\partial x}\right)^2\right] \tag{2a}$$

$$\varepsilon_{yy}=\frac{\partial\bar{u}}{\partial y}+\frac{1}{2}\left[\left(\frac{\partial\bar{u}}{\partial y}\right)^2+\left(\frac{\partial\bar{v}}{\partial y}\right)^2+\left(\frac{\partial\bar{w}}{\partial y}\right)^2\right] \tag{2b}$$

$$\varepsilon_{zz}=\frac{\partial\bar{u}}{\partial z}+\frac{1}{2}\left[\left(\frac{\partial\bar{u}}{\partial z}\right)^2+\left(\frac{\partial\bar{v}}{\partial z}\right)^2+\left(\frac{\partial\bar{w}}{\partial z}\right)^2\right] \tag{2c}$$

$$\gamma_{xy}=\frac{\partial\bar{u}}{\partial y}+\frac{\partial\bar{v}}{\partial x}+\frac{\partial\bar{u}}{\partial y}\frac{\partial\bar{u}}{\partial x}+\frac{\partial\bar{v}}{\partial y}\frac{\partial\bar{v}}{\partial x}+\frac{\partial\bar{w}}{\partial y}\frac{\partial\bar{w}}{\partial x} \tag{2d}$$

$$\gamma_{xz}=\frac{\partial\bar{w}}{\partial x}+\frac{\partial\bar{u}}{\partial z}+\frac{\partial\bar{u}}{\partial z}\frac{\partial\bar{u}}{\partial x}+\frac{\partial\bar{v}}{\partial z}\frac{\partial\bar{v}}{\partial x}+\frac{\partial\bar{w}}{\partial z}\frac{\partial\bar{w}}{\partial x} \tag{2e}$$

$$\gamma_{yz}=\frac{\partial\bar{v}}{\partial z}+\frac{\partial\bar{w}}{\partial y}+\frac{\partial\bar{u}}{\partial y}\frac{\partial\bar{u}}{\partial z}+\frac{\partial\bar{v}}{\partial y}\frac{\partial\bar{v}}{\partial z}+\frac{\partial\bar{w}}{\partial y}\frac{\partial\bar{w}}{\partial z} \tag{2f}$$

($\left(\frac{\partial\bar{u}}{\partial x}\right)^2<<\frac{\partial\bar{u}}{\partial x}$, $\left(\frac{\partial\bar{u}}{\partial y}\right)^2<<\frac{\partial\bar{u}}{\partial y}$, $\left(\frac{\partial\bar{u}}{\partial z}\right)^2<<\frac{\partial\bar{u}}{\partial z}$, $\left(\frac{\partial\bar{u}}{\partial x}\right)\left(\frac{\partial\bar{u}}{\partial y}\right)<<\frac{\partial\bar{u}}{\partial x}+\frac{\partial\bar{u}}{\partial y}$, $\left(\frac{\partial\bar{u}}{\partial x}\right)\left(\frac{\partial\bar{u}}{\partial z}\right)<<\frac{\partial\bar{u}}{\partial x}+\frac{\partial\bar{u}}{\partial z}$, $\left(\frac{\partial\bar{u}}{\partial y}\right)\left(\frac{\partial\bar{u}}{\partial z}\right)<<\frac{\partial\bar{u}}{\partial y}+\frac{\partial\bar{u}}{\partial z}$ i.e. the terms $\left(\frac{\partial\bar{u}}{\partial x}\right)^2$, $\left(\frac{\partial\bar{u}}{\partial y}\right)^2$, $\left(\frac{\partial\bar{u}}{\partial z}\right)^2$, $\left(\frac{\partial\bar{u}}{\partial x}\right)\left(\frac{\partial\bar{u}}{\partial z}\right)$, $\left(\frac{\partial\bar{u}}{\partial x}\right)\left(\frac{\partial\bar{u}}{\partial y}\right)$, and $\left(\frac{\partial\bar{u}}{\partial y}\right)\left(\frac{\partial\bar{u}}{\partial z}\right)$ have been neglected as considered to be small compared with the linear and the rest of the non-linear terms) the strain resultants are given as

$$\underset{6\times1}{\boldsymbol{\varepsilon}}=\underset{6\times171}{\mathbf{D}}\cdot\underset{171\times1}{\mathbf{E}} \tag{3a}$$

where $\boldsymbol{\varepsilon}=\begin{bmatrix}\varepsilon_{xx} & \varepsilon_{yy} & \varepsilon_{yy} & \varepsilon_{xy} & \varepsilon_{xz} & \varepsilon_{yz}\end{bmatrix}^T$ is the strain vector which has been written as a product of two matrices, one ($\mathbf{D}=\mathbf{D}\left(y,z,Y,Z,\varphi_i^j,v_i^j,w_i^j\right)$ where $i=Y,Z,x$ and $j=P,S$) that contains expressions which are functions of the cross sectional coordinates, the warping functions and the components of distortional functions and another ($\mathbf{E} = \mathbf{E}\left(\mathbf{d}, \mathbf{d}_{,x}\right)$) that contains expressions which are functions of the displacements and their derivatives, where $\mathbf{d}^T = \left[u(x),\ v(x),\ w(x),\ \theta_x(x),\ \eta_Y^P(x),\ \eta_Z^P(x),\ \eta_x^P(x),\ \eta_Y^S(x),\ \eta_Z^S(x),\ \eta_x^S(x),\ z_Y^P(x),\ z_Z^P(x),\ z_x^P(x),\ z_Y^S(x),\ z_Z^S(x),\ z_x^S(x)\right]^T$) is the displacement vector. $(\cdot)_{,i}$ denotes differentiation with respect to i.

Considering strains to be small, employing the second Piola-Kirchhoff stress tensor, the stress components are defined in terms of the strain ones as

$$\begin{Bmatrix} S_{xx} \\ S_{yy} \\ S_{zz} \\ S_{xy} \\ S_{xz} \\ S_{yz} \end{Bmatrix} = \begin{bmatrix} 2G+\lambda & \lambda & \lambda & 0 & 0 & 0 \\ \lambda & 2G+\lambda & \lambda & 0 & 0 & 0 \\ \lambda & \lambda & 2G+\lambda & 0 & 0 & 0 \\ 0 & 0 & 0 & G & 0 & 0 \\ 0 & 0 & 0 & 0 & G & 0 \\ 0 & 0 & 0 & 0 & 0 & G \end{bmatrix} \begin{Bmatrix} \varepsilon_{xx} \\ \varepsilon_{yy} \\ \varepsilon_{zz} \\ \gamma_{xy} \\ \gamma_{xz} \\ \gamma_{yz} \end{Bmatrix} \tag{4}$$

or

$$\underset{6\times1}{\mathbf{S}} = \underset{6\times6}{\mathbf{K}_{Material}}\ \underset{6\times1}{\boldsymbol{\varepsilon}} \tag{5}$$

where $G = E/\left(2(1+\nu)\right)$ and $\lambda = \nu E/\left((1+\nu)(1-2\nu)\right)$ are the shear modulus and the Lamé coefficient of the material, respectively. After the substitution of Eqs.(3) in Eqs.(5) the stress vector can be written as

$$\underset{6\times1}{\mathbf{S}} = \underset{6\times6}{\mathbf{K}_{Material}} \cdot \underset{6\times171}{\mathbf{D}} \cdot \underset{171\times1}{\mathbf{E}} \tag{6}$$

2.2 Principle of virtual work

According to principle of virtual work

$$\delta U = \delta W \tag{7}$$

where δU and δW are the virtual work of the internal and external actions of the beam respectively.

2.3 Virtual work of internal actions

The virtual work of the internal actions of beam is given as

$$\delta U = \int_V \left(S_{xx}\delta\varepsilon_{xx} + S_{yy}\delta\varepsilon_{yy} + S_{zz}\delta\varepsilon_{zz} + S_{xy}\delta\gamma_{xy} + S_{xz}\delta\gamma_{xz} + S_{yz}\delta\gamma_{yz} \right) dV = \int_V \left(\underset{1\times6}{\delta\boldsymbol{\varepsilon}^{\mathrm{T}}} \cdot \underset{6\times1}{\mathbf{S}} \right) dV \tag{8}$$

where V is the volume of the beam. Substituting Eqs. (3) and (6) in Eq. (8) the expression of the virtual work of the internal actions can be written as

$$\delta U = \int_0^L \underset{1\times171}{\delta\mathbf{E}^{\mathrm{T}}} \cdot \underset{171\times171}{\mathbf{C}} \cdot \underset{171\times1}{\mathbf{E}}\, dx = \int_0^L \underset{1\times171}{\left(\underset{171\times16}{\frac{\partial \mathbf{E}}{\partial \mathbf{d}}} \cdot \underset{16\times1}{\delta\mathbf{d}} + \underset{171\times16}{\frac{\partial \mathbf{E}}{\partial \mathbf{d}_{,x}}} \cdot \underset{16\times1}{\delta\mathbf{d}_{,x}} \right)^{\mathrm{T}}} \cdot \underset{171\times171}{\mathbf{C}} \cdot \underset{171\times1}{\mathbf{E}}\, dx$$
$$= \int_0^L \underset{1\times171}{\left(\underset{1\times16}{\delta\mathbf{d}^{\mathrm{T}}} \cdot \underset{16\times171}{\left(\frac{\partial \mathbf{E}}{\partial \mathbf{d}}\right)^{\mathrm{T}}} + \underset{1\times16}{\delta\mathbf{d}_{,x}^{\;\mathrm{T}}} \cdot \underset{16\times171}{\left(\frac{\partial \mathbf{E}}{\partial \mathbf{d}_{,x}}\right)^{\mathrm{T}}} \right)} \cdot \underset{171\times171}{\mathbf{C}} \cdot \underset{171\times1}{\mathbf{E}}\, dx = \int_0^L \underset{1\times171}{\left(\underset{1\times32}{\delta\mathbf{d}_{tot}^{\mathrm{T}}} \cdot \underset{32\times171}{\left(\frac{\partial \mathbf{E}}{\partial \mathbf{d}_{tot}}\right)^{\mathrm{T}}} \right)} \cdot \underset{171\times171}{\mathbf{C}} \cdot \underset{171\times1}{\mathbf{E}}\, dx \tag{9a}$$

where

$$\underset{171\times171}{\mathbf{C}} = \int_\Omega \underset{171\times6}{\mathbf{D}^{\mathrm{T}}} \cdot \underset{6\times6}{\mathbf{K}_{Material}} \cdot \underset{6\times171}{\mathbf{D}}\, d\Omega \quad \text{and} \quad \underset{32\times1}{\mathbf{d}_{tot}} = \begin{bmatrix} \underset{16\times1}{\mathbf{d}} \\ \underset{16\times1}{\mathbf{d}_{,x}} \end{bmatrix} \tag{9b}$$

$\mathbf{C}$ is a matrix that contains the non-linear geometric constants of the cross section of the beam.

2.4 Virtual work of external actions

The virtual work of the external actions of beam is given as

$$\delta W = \int_F \left(t_x \delta\overline{u} + t_y \delta\overline{v} + t_z \delta\overline{w} \right) dF = \int_F \left(\underset{1\times3}{\delta\mathbf{u}^{\mathrm{T}}} \cdot \underset{3\times1}{\mathbf{t}} \right) dF = \int_F \left(\underset{1\times3}{\left(\frac{\partial \mathbf{u}}{\partial \mathbf{d}} \delta\mathbf{d} + \frac{\partial \mathbf{u}}{\partial \mathbf{d}_{,x}} \delta\mathbf{d}_{,x} \right)^{\mathrm{T}}} \cdot \underset{3\times1}{\mathbf{t}} \right) dF$$
$$= \int_F \left(\underset{1\times32}{\delta\mathbf{d}_{tot}^{\mathrm{T}}} \cdot \underset{32\times3}{\left(\frac{\partial \mathbf{u}}{\partial \mathbf{d}_{tot}} \right)^{\mathrm{T}}} \cdot \underset{3\times1}{\mathbf{t}} \right) dF \tag{10}$$

where $\mathbf{t}$ is the vector applied on the lateral surface of the beam including end cross sections, denoted by F. After some algebraic manipulations the virtual work of the external actions can be written as

$$\delta W = \int_0^L \left(\sum_{j=1}^{K} \int_{\Gamma_j} \left(\underset{1\times32}{\delta\mathbf{d}_{tot}^{\mathrm{T}}} \cdot \underset{32\times3}{\left(\frac{\partial \mathbf{u}}{\partial \mathbf{d}_{tot}} \right)_j^{\mathrm{T}}} \cdot \underset{3\times1}{\mathbf{t}_j} \right) ds \right) dx$$
$$+ \int_{\Omega^0} \left(\underset{1\times32}{\delta\mathbf{d}_{tot}^{\mathrm{T}}\Big|_{x=0}} \cdot \underset{32\times3}{\left(\frac{\partial \mathbf{u}}{\partial \mathbf{d}_{tot}} \right)^{\mathrm{T}}\Bigg|_{x=0}} \cdot \underset{3\times1}{\mathbf{t}\Big|_{x=0}} \right) d\Omega^0 + \int_{\Omega^L} \left(\underset{1\times32}{\delta\mathbf{d}_{tot}^{\mathrm{T}}\Big|_{x=L}} \cdot \underset{32\times3}{\left(\frac{\partial \mathbf{u}}{\partial \mathbf{d}_{tot}} \right)^{\mathrm{T}}\Bigg|_{x=L}} \cdot \underset{3\times1}{\mathbf{t}\Big|_{x=L}} \right) d\Omega^L \tag{11}$$

2.5 Warping and distortional functions

The calculation of the $\phi_i^j(y,z)$ ($i = Y, Z, x$ and $j = P, S$) warping functions and $v_i^j(y,z)$ and $w_i^j(y,z)$ ($i = Y, Z, x$ and $j = P, S$) components of distortional functions that have been employed in section 2.1 are obtained after solving corresponding boundary value problems, formulated exploiting the local equilibrium equations and the corresponding boundary conditions according to a sequential equilibrium scheme as presented in [4] employing the Boundary Element Method. More specifically, in order to compute the involved warping and distortional functions, local equilibrium is sequentially fulfilled by introducing additional warping and distortional functions, so as to equilibrate non-equilibrated stress residuals [4]. According to sequential equilibrium scheme in each equilibrium stage three deformation modes are added (two due bending about Y and Z axes and one due to torsion about x axis) each of which includes one warping and one distortional function [4]. So the number of degrees of freedom of each node is

$$N_{dofs} = 4 + 2 \cdot \left(3 \cdot N_{stages}\right) \tag{12}$$

where N_{stages} is the number of equilibrium stages that participate in the model. The displacement field that includes up to secondary deformation modes, expressed by Eqs. (1), corresponds to $N_{stages} = 2$ and $N_{dofs} = 16$. If tertiary deformations modes are taken into account it will be $N_{stages} = 3$ and $N_{dofs} = 22$ etc.

3 NUMERICAL SOLUTION

3.1 Shape functions and nodal displacements

According to the proposed analysis, the local buckling problem of homogeneous beams taking into account warping and distortional phenomena due to shear, flexure and torsion is numerically solved employing the Finite Element Method (FEM). According to this method, the displacement components $d_i\left(x\right)$ for $i = 1...16$ (of the displacement vector $\mathbf{d}$) are expressed as a function of nodal displacements and shape functions. An element with two nodes at $x = 0$ and $x = L$ has been employed, where L is the length of the element and the origin of the coordinate system is at its left end. As a result, the aforementioned displacement components are expressed in terms of nodal displacements as

$$d_i\left(x\right) = f_1\left(x\right) \cdot d_{i1} + f_2\left(x\right) \cdot d_{i2} \tag{13a}$$

where d_{i1}, d_{i2} are the nodal displacements of the d_i displacement component at nodes 1 ($x = 0$) and 2 ($x = L$) respectively, while the shape functions $f_1\left(x\right)$, $f_2\left(x\right)$ are given by the expressions

$$f_1\left(x\right) = 1 - \frac{x}{L} \qquad\qquad f_2\left(x\right) = \frac{x}{L} \tag{13b,c,e}$$

that have been calculated in order to hold that $d_i = d_{i1}$ at $x = 0$ and $d_i = d_{i2}$ at $x = L$. Thus, the vector of nodal displacements is defined as

$$\begin{aligned}\mathbf{q} = \Big[& u_1 \quad v_1 \quad w_1 \quad \theta_{x1} \quad \eta_{Y1}^P \quad \eta_{Z1}^P \quad \eta_{x1}^P \quad \eta_{Y1}^S \quad \eta_{Z1}^S \quad \eta_{x1}^S \quad z_{Y1}^P \quad z_{Z1}^P \quad z_{x1}^P \quad z_{Y1}^S \quad z_{Z1}^S \quad z_{x1}^S \;\Big| \\ & \Big|\; u_2 \quad v_2 \quad w_2 \quad \theta_{x2} \quad \eta_{Y2}^P \quad \eta_{Z2}^P \quad \eta_{x2}^P \quad \eta_{Y2}^S \quad \eta_{Z2}^S \quad \eta_{x2}^S \quad z_{Y2}^P \quad z_{Z2}^P \quad z_{x2}^P \quad z_{Y2}^S \quad z_{Z2}^S \quad z_{x2}^S \Big]^T\end{aligned} \tag{14}$$

or

$$\mathbf{q} = [q_1 \quad q_2 \quad q_3 \quad q_4 \quad q_5 \quad q_6 \quad q_7 \quad q_8 \quad q_9 \quad q_{10} \quad q_{11} \quad q_{12} \quad q_{13} \quad q_{14} \quad q_{15} \quad q_{16} \mid \\ \mid q_{17} \quad q_{18} \quad q_{19} \quad q_{20} \quad q_{21} \quad q_{22} \quad q_{23} \quad q_{24} \quad q_{25} \quad q_{26} \quad q_{27} \quad q_{28} \quad q_{29} \quad q_{30} \quad q_{31} \quad q_{32}]^T \tag{15}$$

and the displacement vector can be written as

$$\underset{16\times1}{\mathbf{d}} = \underset{16\times32}{\mathbf{f}} \cdot \underset{32\times1}{\mathbf{q}} \tag{16a}$$

where

$$\underset{16x32}{\mathbf{f}} = \left[\begin{array}{cccc|cccc} f_1(x) & 0 & \cdots & 0 & f_2(x) & 0 & \cdots & 0 \\ 0 & f_1(x) & \cdots & 0 & 0 & f_2(x) & \cdots & 0 \\ \vdots & \vdots & \ddots & \vdots & \vdots & \vdots & \ddots & \vdots \\ 0 & 0 & \cdots & f_1(x) & 0 & 0 & \cdots & f_2(x) \\ & 16x16 & & & & 16x16 & & \end{array} \right] \tag{16b}$$

3.2 Principle of virtual work

Combining Eqs. (7), (9a) and (11) and substituting Eqs. (16a) the principle of virtual work is written as

$$\underset{1\times32}{\delta\mathbf{q}^{\mathrm{T}}} \underset{32\times1}{\mathbf{f}_s} = \underset{1\times32}{\delta\mathbf{q}^{\mathrm{T}}} \underset{32\times1}{\mathbf{P}} \tag{17}$$

or

$$\underset{32\times1}{\mathbf{f}_s} = \underset{32\times1}{\mathbf{P}} \tag{18}$$

where $\mathbf{f}_s$ and $\mathbf{P}$ are the elastic forces and the load vector respectively.

3.3 Elastic forces

Substituting Eqs. (16a) in Eq. (9a) the expression of the virtual work of the internal actions can be written as

$$\delta U = \underset{1\times32}{\delta\mathbf{q}^{\mathrm{T}}} \int_0^L \underset{32\times171}{\mathbf{Z}^{\mathrm{T}}} \cdot \underset{171\times171}{\mathbf{C}} \cdot \underset{171\times1}{\mathbf{E}} \, dx \tag{19a}$$

where

$$\underset{171\times32}{\mathbf{Z}} = \underset{171\times32}{\frac{\partial \mathbf{E}}{\partial \mathbf{d}_{tot}}} \underset{32\times32}{\mathbf{f}_{tot}} \quad \text{and} \quad \underset{32\times32}{\mathbf{f}_{tot}} = \begin{bmatrix} \underset{16\times32}{\mathbf{f}} \\ \underset{16\times32}{\mathbf{f}_{,x}} \end{bmatrix} \tag{19b}$$

So the developing elastic forces are evaluated as

$$\underset{32\times 1}{\mathbf{f}_s} = \int_0^L \underset{32\times 171}{\mathbf{Z}^{\mathrm{T}}} \cdot \underset{171\times 171}{\mathbf{C}} \cdot \underset{171\times 1}{\mathbf{E}}\, dx \tag{20}$$

3.4 Load vector

Substituting Eqs. (16a) in Eq. (11) the expression of the virtual work of the external actions can be written as

$$\delta W = \underbrace{\underset{1\times 32}{\delta\mathbf{q}^{\mathrm{T}}} \int_0^L \left(\sum_{j=1}^{K} \int_{\Gamma_j} \left(\underset{32\times 3}{\mathbf{H}_j^{\mathrm{T}}} \cdot \underset{3\times 1}{\mathbf{t}_j} \right) ds \right) dx}_{\text{Lateral Surface}} + \underbrace{\underset{1\times 32}{\delta\mathbf{q}^{\mathrm{T}}} \int_{\Omega^0} \left(\underset{32\times 3}{\mathbf{H}^{\mathrm{T}}\Big|_{x=0}} \cdot \underset{3\times 1}{\mathbf{t}\Big|_{x=0}} \right) d\Omega^0}_{\text{Left end } (x=0)} + \underbrace{\underset{1\times 32}{\delta\mathbf{q}^{\mathrm{T}}} \int_{\Omega^L} \left(\underset{32\times 3}{\mathbf{H}^{\mathrm{T}}\Big|_{x=L}} \cdot \underset{3\times 1}{\mathbf{t}\Big|_{x=L}} \right) d\Omega^L}_{\text{Right end } (x=L)} \tag{21a}$$

where

$$\underset{3\times 32}{\mathbf{H}} = \underset{3\times 32}{\frac{\partial \mathbf{u}}{\partial \mathbf{d}_{tot}}} \underset{32\times 32}{\mathbf{f}_{tot}} \tag{21b}$$

or

$$\delta W = \underset{1\times 32}{\delta\mathbf{q}^{\mathrm{T}}} \int_0^L \underset{32\times 1}{\mathbf{p}}\, dx + \underset{1\times 32}{\delta\mathbf{q}^{\mathrm{T}}} \underset{32\times 1}{\mathbf{P}_0} + \underset{1\times 32}{\delta\mathbf{q}^{\mathrm{T}}} \underset{32\times 1}{\mathbf{P}_L} \tag{22a}$$

where

$$\underset{32\times 1}{\mathbf{p}} = \sum_{j=1}^{K} \left(\int_{\Gamma_j} \left(\underset{32\times 3}{\mathbf{H}_j^{\mathrm{T}}} \cdot \underset{3\times 1}{\mathbf{t}_j} \right) ds \right) \qquad \underset{32\times 1}{\mathbf{P}_0} = \int_{\Omega^0} \left(\underset{32\times 3}{\mathbf{H}^{\mathrm{T}}} \cdot \underset{3\times 1}{\mathbf{t}} \right)\Bigg|_{x=0} d\Omega^0 \qquad \underset{32\times 1}{\mathbf{P}_L} = \int_{\Omega^L} \left(\underset{32\times 3}{\mathbf{H}^{\mathrm{T}}} \cdot \underset{3\times 1}{\mathbf{t}} \right)\Bigg|_{x=L} d\Omega^L \tag{22b,c,d}$$

$\mathbf{p}$ is the distributed load vector over the length of the beam while $\mathbf{P}_0$ and $\mathbf{P}_L$ are the concentrated loads applied at the left ($x = 0$) and at the right ($x = L$) end of the beam, respectively. So the load vector is evaluated as

$$\underset{32\times 1}{\mathbf{P}} = \int_0^L \underset{32\times 1}{\mathbf{p}}\, dx + \underset{32\times 1}{\mathbf{P}_0} + \underset{32\times 1}{\mathbf{P}_L} \tag{23}$$

3.5 Element stiffness matrix

Eqs. (18), that have to be solved, can be written as

$$\underset{32\times 1}{\mathbf{f}_s} - \underset{32\times 1}{\mathbf{P}} = \underset{32\times 1}{\mathbf{0}} \tag{24}$$

or

$$\underset{32\times32}{\mathbf{K}}\ \underset{32\times1}{\delta\mathbf{q}} = \underset{32\times1}{\mathbf{0}} \tag{25}$$

where $\mathbf{K}$ is the total stiffness matrix of the element that is calculated employing the expression

$$\underset{32\times32}{\mathbf{K}} = \underset{32\times32}{\frac{\partial\mathbf{f}_s}{\partial\mathbf{q}}} - \underset{32\times32}{\frac{\partial\mathbf{P}}{\partial\mathbf{q}}} \tag{26}$$

after the substitution of Eqs.(20), (22b-d) and (23) the stiffness matrix is obtained as

$$\underset{32\times32}{\mathbf{K}} = \underset{32\times32}{\mathbf{K}_{\mathbf{f}_s}} - \underset{32\times32}{\mathbf{K}_{\mathbf{P}}} \tag{27a}$$

where

$$\underset{32\times32}{\mathbf{K}_{\mathbf{f}_s}} = \int_0^L \underset{32\times171}{\mathbf{Z}^{\mathrm{T}}} \cdot \underset{171\times171}{\mathbf{C}} \cdot \underset{171\times32}{\mathbf{Z}}\, dx + \int_0^L \sum_{i=1}^{171} \underset{1\times1}{\mathbf{CE}(i)} \cdot \underset{32\times32}{\mathbf{f}_{tot}^{\mathrm{T}}} \underbrace{\frac{\partial}{\partial \underset{32\times1}{\mathbf{d}_{tot}}}\left(\frac{\partial \mathbf{E}}{\partial \underset{32\times1}{\mathbf{d}_{tot}}}^{\mathrm{T}} (:,i) \right)}_{32\times32} \cdot \underset{32\times32}{\mathbf{f}_{tot}}\, dx \tag{27b}$$

$$\mathbf{K}_{\mathbf{P}} = \int_0^L \sum_{j=1}^{K} \underset{32\times32}{\left(\int_{\Gamma_j} \frac{\partial}{\partial \underset{32\times1}{\mathbf{d}_{tot}}} \left(\underset{32\times3}{\mathbf{H}_j^{\mathrm{T}}} \cdot \underset{3\times1}{\mathbf{t}_j} \right) ds \right)} \cdot \underset{32\times32}{\mathbf{f}_{tot}}\, dx +$$

$$+ \int_{\Omega^0} \left. \left(\frac{\partial}{\partial \underset{32\times1}{\mathbf{d}_{tot}}} \left(\underset{32\times3}{\mathbf{H}^{\mathrm{T}}} \cdot \underset{3\times1}{\mathbf{t}} \right) \right) \right|_{x=0} d\Omega^0 + \int_{\Omega^L} \left. \left(\frac{\partial}{\partial \underset{32\times1}{\mathbf{d}_{tot}}} \left(\underset{32\times3}{\mathbf{H}^{\mathrm{T}}} \cdot \underset{3\times1}{\mathbf{t}} \right) \right) \right|_{x=L} d\Omega^L \tag{27b}$$

$$\underset{171\times1}{\mathbf{CE}} = \underset{171\times171}{\mathbf{C}} \cdot \underset{171\times1}{\mathbf{E}} \tag{27b}$$

The stiffness matrix can be written as

$$\underset{32\times32}{\mathbf{K}} = \underset{32\times32}{\mathbf{K}_{lin}} + \underset{32\times32}{\mathbf{K}_{nl}} \tag{28}$$

where $\mathbf{K}_{lin}$ (the linear part) can be calculated by substituting $\mathbf{q} = \mathbf{0}$ in Eqs. (27) and $\mathbf{K}_{nl}$ (the nonlinear part) by Eqs. (27) as $\mathbf{K}_{nl} = \mathbf{K} - \mathbf{K}_{lin}$ and after substituting $\cos(\theta_x) = 1 - \theta_x^2/2$ and $\sin(\theta_x) = \theta_x - \theta_x^3/6$ and preserving non-linear terms up to 1st order.

3.6 Total stiffness matrix and buckling criterion

Separating the beam in N elements, employing the direct stiffness method and taking into account the boundary conditions of the beam, the total system of equations is formulated as

$$\left(\mathbf{K}_{lin}^{tot} + \lambda \cdot \mathbf{K}_{nl}^{tot}\right)\delta\mathbf{q}^{tot} = \mathbf{0} \tag{29}$$

The buckling load is calculated by the solution of the generalized eigenvalue problem of Eqs. (29) where $\mathbf{K}_{lin}^{tot}$ is the linear stiffness matrix of the beam and $\mathbf{K}_{nl}^{tot}$ is calculated for $\mathbf{q} = \mathbf{q}_0$ which is calculated by the solution of the linear problem

$$\mathbf{q}_0 = \mathbf{K}_{lin}^{-1} \cdot \mathbf{P}_{lin} \tag{30}$$

where $\mathbf{P}_{lin}$ is calculated by substituting $\mathbf{q} = \mathbf{0}$ in Eqs. (23). The eigenvalues λ represent the load factor that multiply $\mathbf{P}_{lin}$ and leads beam to buckle. So load vector that causes buckling is

$$\mathbf{P}_{cr} = \lambda \cdot \mathbf{P}_{lin} \tag{31}$$

and the eigenvectors $\delta\mathbf{q}_{cr}^{tot}$ are the corresponding modeshapes.

4 NUMERICAL EXAMPLE

In order to investigate the influence of distortional phenomenon in linear buckling analysis of beams, a numerical example drawn from the literature [5, 6] is examined. Closed cross section cantilever beams (Figure 2a), for length varying from $L = 5.0m$ to $L = 40.0m$, with a homogeneous ($E = 10^6 kN/m^2$, $\nu = 0.25$) rectangular cross section (Figure 2b**)** have been analysed. More specifically, the buckling load has been calculated employing Distortional Beam Theory (present study) for varying number of degrees of freedom of each node (N_{dofs}) with 40 FE and is compared with the corresponding results according to Generalized Warping Beam Theory (GWBT) with 41 FE (takes into account shear lag both due to flexure and torsion, distortion is not taken into account) [5], Euler - Bernoulli Beam Theory including primary torsional warping (E/BBT) employing 41 FE [5], Timoshenko Beam Theory taking into account primary torsional warping (TBT) employing 50 FE [5], Solid FEM without diaphragms (w/out d.) [5] and solid FEM with diaphragms (with d.) [5]. In this example in the Solid FEM with d. model rigid diaphragms in each set of nodes having the same longitudinal coordinate have been employed, pointing out that the diaphragms are designed so as each set of nodes has the same translation and rotation in the cross section plane, corresponding to that cross section maintains its shape at the transverse directions during deformation (distortion is not taken into account –assumption of E/EBT, TBT, GWBT). In both solid FEM models 1200 solid FE per meter of length have been employed [5]. The aforementioned results are compared with those calculated by Wang and Li [6] which calculated the buckling loads of thin walled members taking into account shear lag effect (distortion is not taken into account). Figure 2c shows the aforementioned buckling loads.

The discrepancies between Solid FEM with d. and Solid FEM w/out d. as well as those between GWBT and DBT for $N_{dofs} = 34$ show that for the lengths where the two solutions are different local buckling is dominant. Comparing DBT results with those obtained by Solid

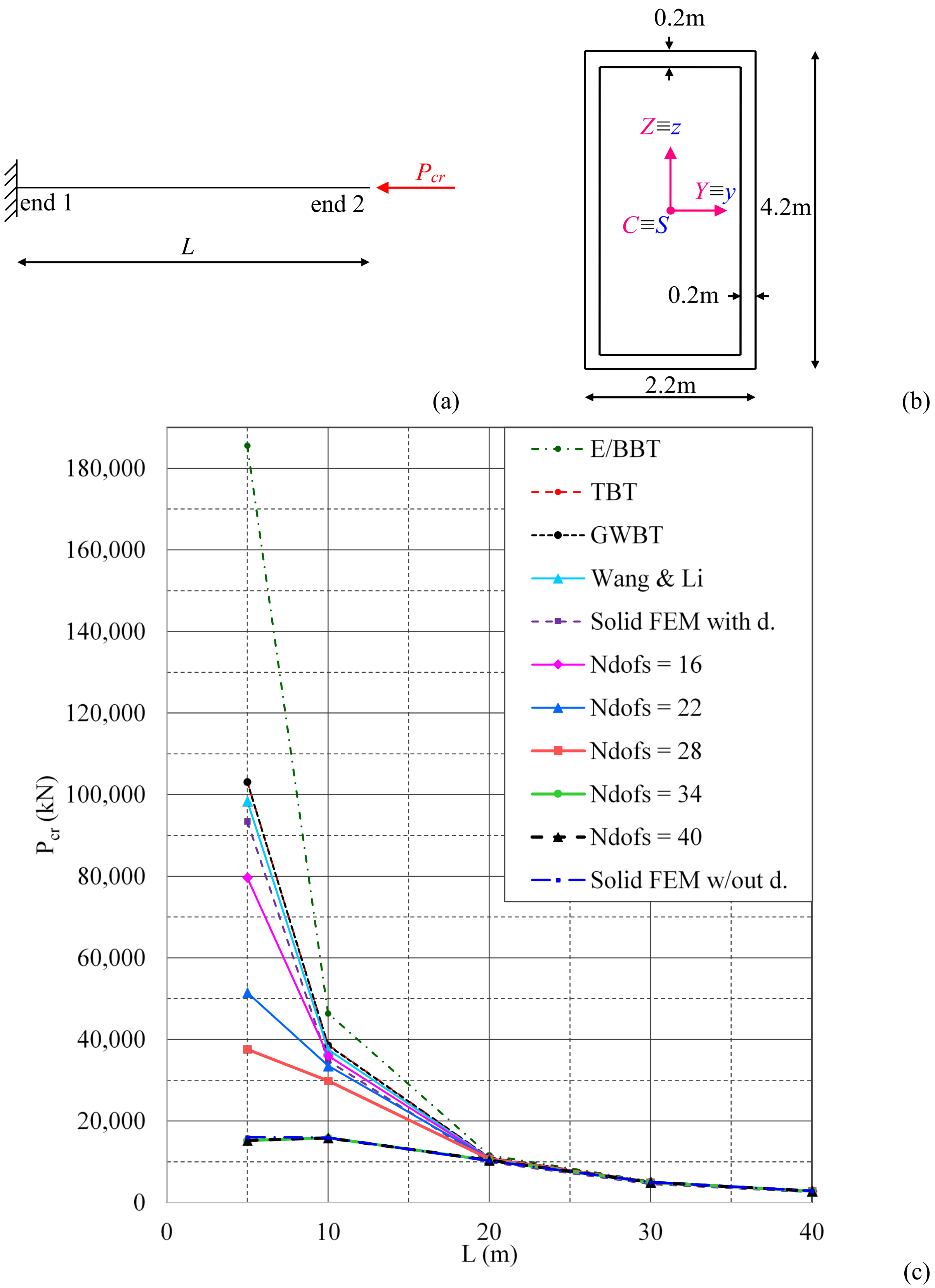

Figure 2: Boundary conditions and loading (a), cross section (b) and buckling loads of beams of numerical example as obtained from E/BBT [5], TBT[5], GWBT [5], Solid FEM with and without diaphragms [5], Wang and Li [6] and DBT (present study) for various N_{dofs}(c).

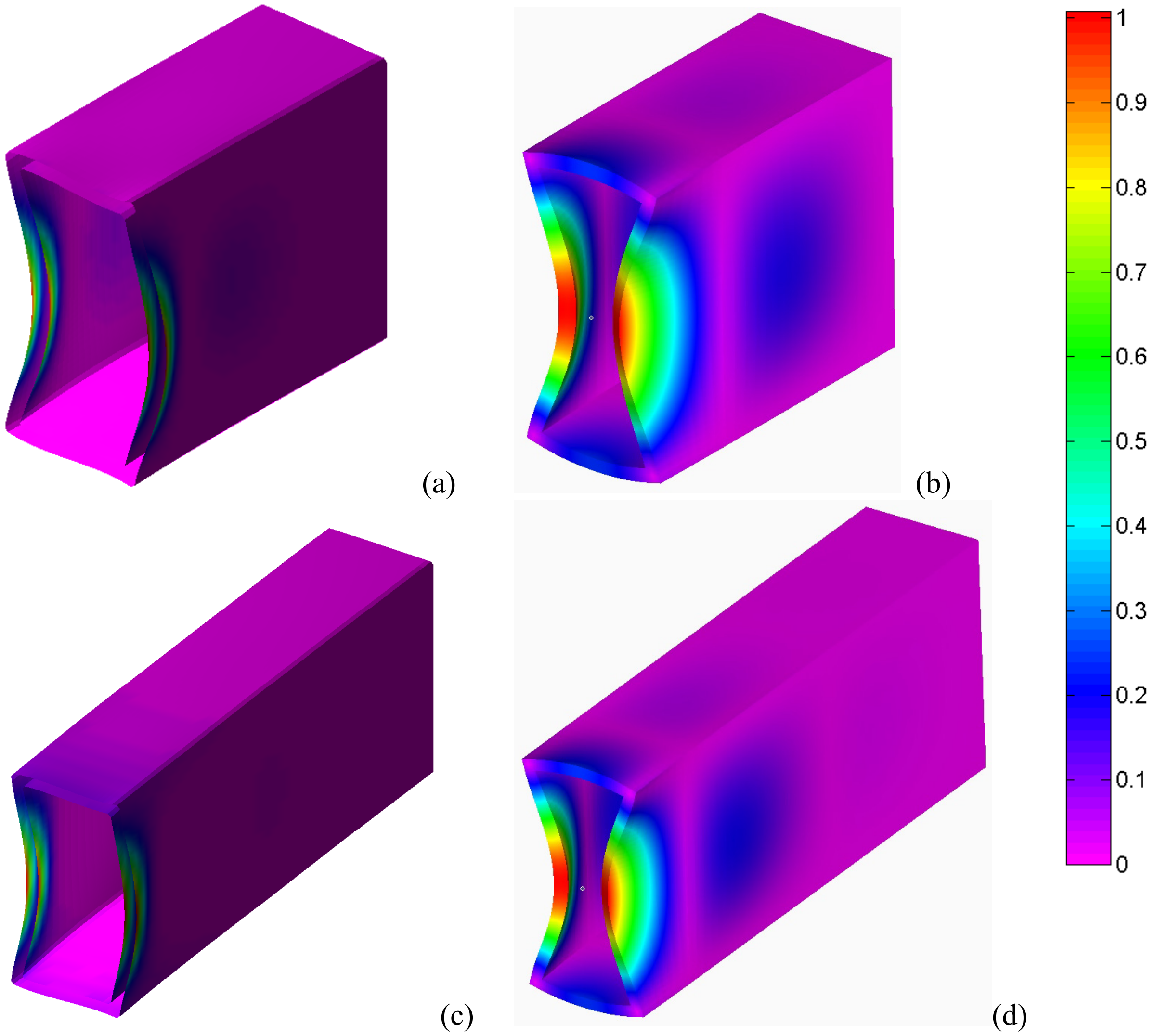

Figure 3: Modeshape for $L=5m$ (a, b) and $L=10m$ (c, d) as calculated by DBT (present study) for $N_{dofs}=34$ and Solid FEM without diaphragms, respectively.

FEM w/out d. it is obvious that as the N_{dofs} increases DBT results approach Solid FEM w/out d. solution. Especially for N_{dofs} equal to 34 and 40 the results are almost the same, so can be concluded that DBT (proposed method) convergences and that for sufficient N_{dofs} DBT can give as accurate results as Solid FEM w/out d. even in cases of short lengths (e.g. $\frac{\text{Beam Length}}{\text{longest side of the cross section}}=1.19$ for $L=5m$) where local buckling dominates (Figure 3a,b). The buckling load calculated from DBT for $N_{dofs}=34$, solid FEM w/out d. and solid FEM with d. for $L=5m$ is P_{cr}^{DBT}=15,224.01kN , $P_{cr}^{Solid\ FEM\ w/out\ d.}$=16,030.75kN and $P_{cr}^{Solid\ FEM\ with\ d.}$=93,440.91kN respectively. So it holds $\frac{P_{cr}^{DBT}-P_{cr}^{Solid\ FEM\ w/out\ d.}}{P_{cr}^{Solid\ FEM\ w/out\ d.}}=-5\%$ and

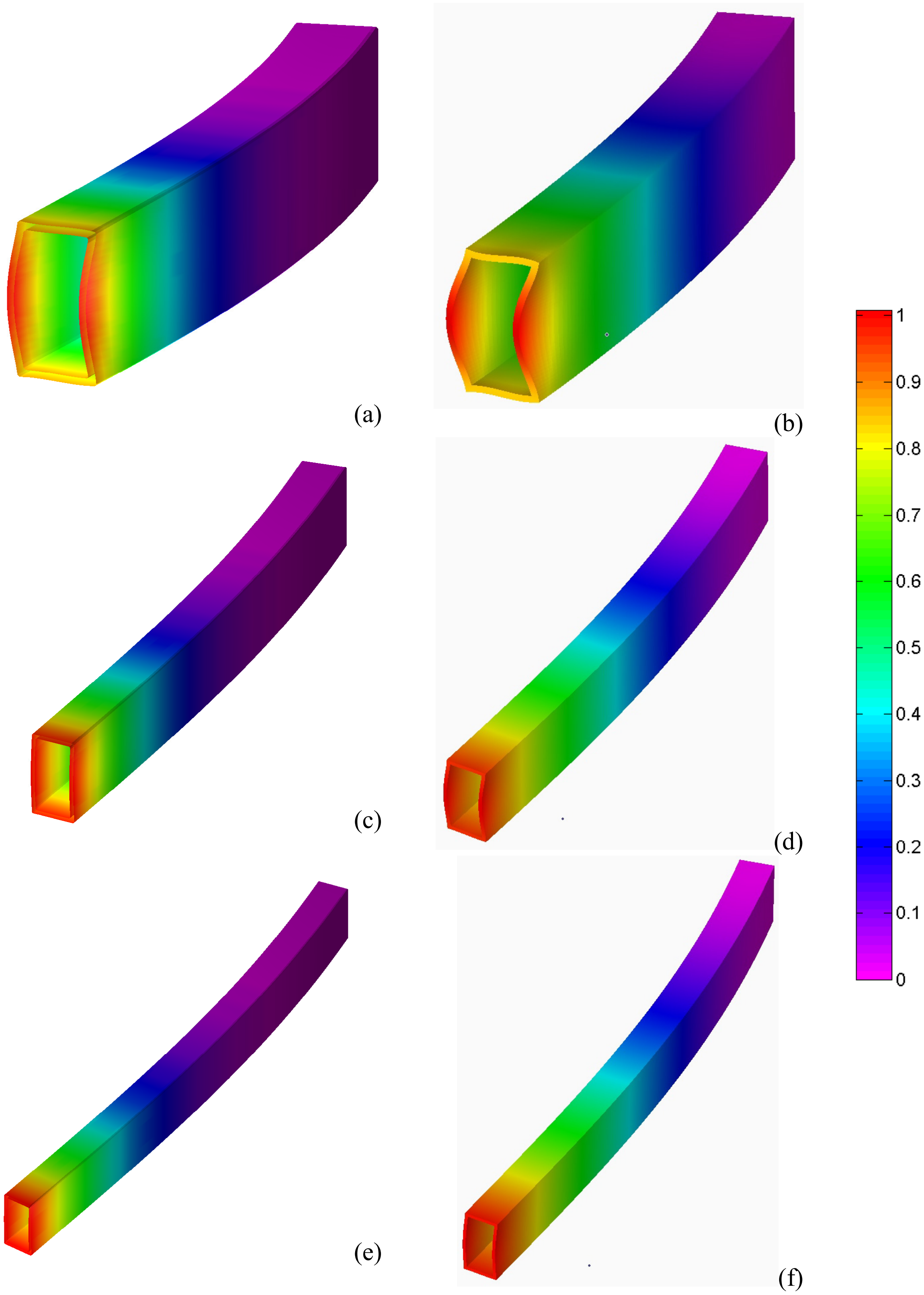

Figure 4: Modeshape for $L = 20m$ (a, b), $L = 30m$ (c, d) and $L = 40m$ (e, f) as calculated by DBT (present study) for $N_{dofs} = 34$ and Solid FEM without diaphragms, respectively.

$\frac{\mathrm{P}_{cr}^{Solid\ FEM\ with\ d.}-\mathrm{P}_{cr}^{Solid\ FEM\ w/out\ d.}}{\mathrm{P}_{cr}^{Solid\ FEM\ w/out\ d.}}=482\%$. From these comparisons is apparent the great importance of the distortional phenomenon in buckling analysis of beams.

Figure 3 presents the buckling modeshapes for $L=5m$ (Figure 3a,b) and $L=10m$ (Figure 3 c,d) as calculated by DBT for $N_{dofs}=34$ and Solid FEM without diaphragms, respectively. It is obvious that these modeshapes correspond to local buckling which is consistent with the fact that the buckling loads of GWBT and DBT for $N_{dofs}=34$ are not the same. Comparing DBT with solid FEM w/out d. results can be concluded that the respective modeshapes are not identical, as expected, because in present DBT model warping and distortional degrees of freedom related with axial loading are not included. This will be accomplished in a future research effort.

Figure 4 presents the buckling modeshapes for $L=20m$ (Figure 4a,b), $L=30m$ (Figure 4c,d) and $L=40m$ (Figure 4e,f) as calculated by DBT for $N_{dofs}=34$ and Solid FEM without diaphragms, respectively. It is obvious that these modeshapes correspond to global buckling, which is consistent with the fact that the buckling loads of GWBT and DBT for $N_{dofs}=34$ are approximately the same. Comparing DBT with solid FEM w/out d. results can be concluded that the respective modeshapes are identical.

5 CONCLUSIONS

In this paper, the a higher order beam element is employed for local buckling analysis of beams of arbitrarily shaped, homogeneous cross-section, taking into account warping and distortional phenomena due to shear, flexure and torsion. The beam is subjected to arbitrary axial, transverse and/or torsional concentrated or distributed load, while its edges are restrained by the most general linear boundary conditions. The main conclusions that can be drawn from this investigation are as follows:

- Distortional phenomenon has great influence in the calculation of the linear buckling load.
- Local buckling is dominant for small values of $\frac{\text{Beam Length}}{\text{longest side of the cross section}}$ so distortional phenomenon is needed to be taken into account in buckling analysis of beam members.
- DBT (proposed method) convergences for increasing N_{dofs}.
- For sufficient N_{dofs} DBT can give as accurate results as Solid FEM w/out d. even in cases of short lengths where local buckling dominates.
- The inclusion of warping and distortional degrees of freedom related with axial loading is considered as necessary in order to calculate the right modeshapes in cases where local buckling is dominant. This will be accomplished in a future research effort.

6 ACKNOWLEDGEMENTS

This research work was supported by “Onassis Foundation”, “Foundation for Education and European Culture” and “A.G. Leventis Foundation”.

REFERENCES

[1] E. Reissner, Analysis of shear lag in box beams by the principle of minimum potential energy. *Q. Appl. Math.*, **41**, 268 – 278, 1946.

[2] R. Schardt, Lateral Torsional and Distortional Buckling of Channel- and Hat-Sections. *Journal of Constructional Steel Research*, **31**, 243-265,1994b.

[3] E.J. Sapountzakis, J.A. Dourakopoulos, Flexural – Torsional Buckling Analysis of Composite Beams by BEM Including Shear Deformation Effect. *Mechanics Research Communications*, **35**, 497-516, 2008.

[4] I.C. Dikaros and E.J. Sapountzakis. Distortional Analysis of Beams of Arbitrary Cross Section by BEM. *Journal of Engineering Mechanics,* ASCE, in print, 2017.

[5] A.K. Argyridi and E.J. Sapountzakis, Generalized Warping In Flexural-Torsional Buckling Analysis of Composite Beams. *Journal of Applied and Computational Mechanics*, **2** (3),152-173, 2016.

[6] Q. Wang, W.Y. Li, Buckling of thin-walled compression members with shear lag using spline finite member element method. *Computational Mechanics*, **18**, 139-146, 1996.